

# RXTE observation of PSR B1706-44 and implications for theoretical models of pulsar emission

A. Ray <sup>1</sup>, A.K. Harding

NASA/Goddard Space Flight Center, Greenbelt, MD 20771

M. Strickman

Naval Research Laboratory, Space Sciences Division, Washington, D.C. 20375

## ABSTRACT

We report on results of an observation with the Rossi X-Ray Timing Explorer (RXTE) of PSR B1706-44 with a live time of 132 ks, to search for pulsed X-ray emission. PSR B1706-44 is a radio and high-energy gamma-ray pulsar (detected by EGRET), but no pulsed emission has been detected in the X-ray band. Since most of the other known gamma-ray pulsars emit pulsed X-rays, it is expected that PSR B1706-44 would also be an X-ray pulsar. However, while the ROSAT PSPC detected a source at the pulsar position, it did not detect pulsations, giving a pulsed fraction upper limit of 18%. The RXTE observations to search for modulation at the pulsar period were carried out in November 1996 and May 1997 during the low states of the nearby X-ray binary 4U1705-44. No significant modulation was detected at the pulsar period, giving an upper limit of  $10^{-6}$  photons  $\text{cm}^{-2} \text{s}^{-1} \text{keV}^{-1}$  in the interval  $9 \text{ keV} \leq E \leq 18.5 \text{ keV}$ . The implications of this upper limit of the pulsed flux from the RXTE observation, taken together with multiband observations of this pulsar are examined in the context of theoretical models of pulsar particle acceleration zones and associated high energy electromagnetic emission.

*Subject headings:* stars:neutron – pulsars:general – pulsars:individual: PSR B1706-44 – X-rays:stars

## 1. Introduction

In recent years multiwavelength observations of several pulsars are now allowing the testing and refinement of theoretical models of pulsar emission mechanisms and particle acceleration responsible for high energy electromagnetic radiation. There are now seven pulsars (eight if PSR0656+14 is counted) which are to emit *pulsed* gamma-rays observed by the EGRET instrument

---

<sup>1</sup>On leave of absence from: Tata Institute of Fundamental Research, Mumbai 400005, India; E-mail: akr@tifrvax.tifr.res.in

aboard the Compton Gamma-ray Observatory (CGRO) (see Thompson et al 1997), . In addition there are more than two dozen isolated (rotation powered) neutron stars which are detected by a number of X-ray satellites such as Einstein, ROSAT and ASCA (see e.g. Becker and Trümper 1997). Spectra, pulse shapes, relative arrival times of pulses in different electromagnetic bands and, in some cases, phase resolved spectra offer information which can be useful for identifying the zone of acceleration of the charged particles in the magnetosphere surrounding the pulsar, and the way these particles produce and interact with electromagnetic radiation. However, of the seven gamma-ray pulsars identified, only six have detected pulsations in the X-ray band, and only five (Crab, Vela, Geminga, PSR1055-52 and PSR1951+32) have measured X-ray spectra. No X-ray pulsations have been detected from the gamma-ray pulsar PSR B1706-44, although steady X-ray emission has been seen by ROSAT from this object. Additionally, ASCA has taken spectral data of the nebular emission surrounding the pulsar and a combined analysis of this and the higher spatial resolution (single-band) ROSAT HRI data has been performed by Finley et al (1998).

PSR B1706-44 is a young neutron star (spin down age  $1.75 \times 10^4$  yr) with a spin period of 0.102 s and has a large spin down luminosity of  $3.4 \times 10^{36}$  erg s<sup>-1</sup> at a distance of 1.82 kpc. The pulsar which was originally discovered in the radio band by Johnston et al (1992), ranks fourth in a rank ordered list of spin-down flux ( $I\Omega\dot{\Omega}/D^2$ ). The soft X-ray emission was detected by the ROSAT PSPC (Becker et al 1992) with an upper limit to modulation of the X-ray flux at the 18% level (Becker, Brazier and Trumper 1995). As most gamma-ray pulsars emit pulsed X-rays, it is of interest to detect the X-ray pulsations from this high spin-down flux pulsar and to study its pulsed spectrum. In this paper we report on our attempt to detect X-ray pulsations from this pulsar using the Rossi X-ray Timing Explorer (RXTE). Preliminary results from this observation were reported by Ray, Harding and Strickman (1997). Although we have not detected any X-ray pulsations, the stringent upper limit to the pulsed flux we obtained has implications for magnetospheric particle acceleration and radiation models. In section 2, we describe the characteristics of PSR B1706-44 and the theoretical motivations for this study. In section 3, we describe the observation carried out with RXTE and its analysis. In section 4, we compare the broadband observations of this pulsar with the theoretical models of the pulsed radiation mechanism in the light of our new observation. In section 5, we discuss our conclusions.

## 2. Motivation for pulse detection and characteristics of PSR 1706-44

X-ray emission from rotation powered pulsars can be a combination of varying amounts of three spectral components: 1) a soft blackbody 2) a power law and 3) a hard component connected with heated polar caps. Blackbody-like emission seen at energies between 0.1 and 0.5 keV can result from surface cooling of the neutron star. Polar cap heating by energetic particles or internal sources may produce a second thermal component at higher energies.. A power-law component could result from non-thermal radiation of particles accelerated in the pulsar magnetosphere.

Measurement of the pulsed X-ray flux from polar cap heating can act as a calorimeter of the

returned particle flux from a polar cap (PC) or outer gap (OG) vacuum discharge accelerator. The returned particle flux is an indicator of the properties and mechanisms of the non-thermal (gamma-ray and power law X-ray) emission from the pulsar. In particular PC models predict a returned flux that is a small percentage of the total accelerated particle flux (Harding and Muslimov 1998 (HM98), Arons 1981) whereas the OG models predict roughly equal numbers of particles accelerated towards the PC as flowing away (Halpern and Ruderman 1993; Wang et al 1998 (hereafter WRHZ)). The latter, therefore, would give rise to comparable X-ray and gamma-ray photon fluxes. These measurements for pulsars could serve as an important separator of the two classes of models.

At present, it is not clear how and where in the pulsar magnetosphere the pulsed non-thermal high energy emission originates. Polar cap models assume that particles are accelerated above the neutron star surface and that radiation results from a curvature radiation (Daugherty and Harding 1996) or inverse-Compton (Sturmer and Dermer 1994) induced pair cascade in a strong magnetic field. Outer-gap models (Cheng, Ho and Ruderman, 1986; CHRa,b) assume that acceleration occurs along null charge surfaces in the outer magnetosphere and that the radiation results from curvature radiation/photon-photon pair production cascades (Ray and Benford 1981). The computed spectra of the pulsars in both polar cap (DH96) and outer-gap (Ho 1989) models predict that the spectrum will extend below 50 keV. In polar cap models this emission is primarily power-law synchrotron emission that will terminate at the cyclotron energy of the local magnetic field, which could be anywhere from  $\sim 10$  keV at the neutron star surface down to  $\sim 0.1$  keV several stellar radii above the surface. A measurement of the pulsed emission below 50 keV would determine how far the spectrum of the non-thermal component extends. If a cutoff in the spectrum is observed, it might be a measure of the local field strength in the emission region and thus, a limit of the proximity of a polar cap cascade to the neutron star surface.

The seven gamma-ray pulsars detected by the Compton Gamma-ray Observatory have high spin down luminosities and, because of their association with EGRET gamma-ray sources, probably have pulsed X-ray fluxes. In the case of PSR B1706-44 there is not enough spectral information to classify the emission as thermal vs non thermal nor determine whether any fraction is pulsed. ROSAT has made pointed observations of this pulsar on three different occasions with both the PSPC (Feb 1992 and Sept 1992 – see Becker et al 1995) and the HRI (Mar 1995 – see Finley et al 1998) for 11.8 ks and 28 ks respectively. The former showed a net count rate of  $0.022 \pm 0.002$  cps for the energy range 0.1 - 2.4 keV. The net count rate reported by HRI was 0.0087 cps which was considered consistent with the PSPC count rate. The HRI-determined J2000 source location was in good agreement with the previous radio (interferometric and timing) positions of Frail et al (1994) and Johnston et al (1992). In addition, ASCA SIS and GIS instruments imaged the region around PSR B1706-44 for net exposures of 20 and 23 ks respectively on 10 Sept 1994 with reported net count rates of 0.016 and 0.018 cps respectively. While the  $2\sigma$  upper limit of the pulsed fraction is 18% in the ROSAT PSPC band, the upper limit for the ASCA band gives a 22% limit in the 2.0-10.0 keV band at a 99% confidence level. The size of the synchrotron nebula (to

the flux levels searched by ROSAT HRI) was found to be  $27''$  in radius (Finley et al. 1998).

Spectral analysis of ROSAT PSPC data did not distinguish between black body and power law models, but the lack of pulsations and the similarity of spin parameters of PSR B1706-44 with those of Vela were used by Becker et al. (1995) to favor a power law model with  $dN/dE \propto E^{-2.4}$  which suggested synchrotron emission from a pulsar powered nebula as the likely origin of detected (steady) X-rays. The corresponding neutral hydrogen column depth  $N_H$  was required to be  $5.4 \times 10^{21} \text{cm}^{-2}$  from spectral fits. The flux within the 0.1-2.4 keV range and the bolometric luminosity (isotropic) at a distance of 1.8 kpc are about  $3.2 \times 10^{-12} \text{erg s}^{-1} \text{cm}^{-2}$  and  $1.3 \times 10^{33} \text{erg s}^{-1}$  respectively. The energy spectra obtained with ASCA SIS and GIS are well fit by a single power law model which gives a photon index  $\alpha = 1.7_{-0.4}^{+0.5}$  and  $N_H = 1.9 \times 10^{21} \text{cm}^{-2}$  with  $L(2-10 \text{keV}) = 5.3 \times 10^{32} \text{erg s}^{-1} \text{cm}^{-2}$ .

The bright Low Mass X-ray Binary 4U 1705-44 is about  $22'$  away from PSR B1706-44 (see Fig 1). In addition there is a faint source in soft X-ray band at  $RA = 17^h 10^m 44^s$   $DEC = -44^\circ 33' 28''$ . These two sources cause confusion and background problems for RXTE since they are all within the FWHM response circle of the RXTE PCA detector. Additionally, the large scattering wings of the ASCA mirrors mean that flux from these sources contributes to the ASCA background for PSR B1706-44.

The EGRET instrument shows a photon spectral index of  $1.57 \pm 0.05$  in the gamma-ray energy range of 100 MeV to 2 GeV for this pulsar and steepens at higher energies (Fierro 1995). In addition there are upper limits to the optical (R-band) magnitude of this pulsar which are discussed together with multiband observations in the context of theoretical models in Section 4.3.

### 3. RXTE Observation & Analysis

PSR B1706-44 was observed as an RXTE Target of Opportunity (TOO) when the nearby bright LMXB 4U 1705-44, went into a low state (corresponding to 5 ct/s in the All Sky Monitor). This LMXB, which is about  $22'$  away from PSR B1706-44, remains in the FOV of the PCA instrument and is therefore a source of contamination which reduces the available pulsed signal to noise. Hence it is advantageous to perform the experiment to detect pulsations when the LMXB is in a low state. A gray-scale image of the region of the sky downloaded from the High Energy Astrophysics Archive (HEASARC) with a superimposed circle denoting the XTE PCA HWHM radius is shown in Figure 1.

PSR B1706-44 was allocated 147 ksec of TOO observation. It was observed on two different occasions between November 9-12, 1996 and May 16-19, 1997. The dates, instrument configurations, exposures etc., are listed in Table 1. After excising the times of SAA passage and earth occultations etc., the on-source live time was 132 ks. During this time all 5 Proportional Counter Units (PCU) were kept on. On certain occasions, the nearby LMXB 4U1705-44 underwent

type I X-ray bursts, enhancing its luminosity by several orders of magnitude for a few tens to a hundred seconds even though generally, the LMXB was in a quasiperiodic low state (as seen by the All Sky Monitor as referred to above) for  $\sim 20$  days. Several hundred seconds of data, comprising the bursts and a roughly equal amount of time immediately after each burst were excluded from our timing analysis for PSR B1706-44 X-ray pulse detection by visually examining the Standard2 light curves and then using the ftools software package *grosstimefilt*.

A preliminary investigation of the data revealed that the average count rate in channels 5-22 (in GoodXenon-16s mode) was substantially higher than that in channels 23-49. It is also well known that the instrumental background in channels 49 through 255 usually is too high to make low signal to noise detections of pulsed emission feasible. Hence we divided the data into bands containing channels 5 through 22 and 23 through 49 and used mainly the latter set of channels for timing analysis towards pulse detection because the contaminating emission from the LMXB was lower in these channels. For the span of data which was of the mode EA-125us-64M-0-1s in November 1996, we chose the appropriate channel boundaries (CPIX4) which corresponded to the same range of energy as the chosen channels (23-49) for the GoodXenon mode, for a combined analysis.

In order to ameliorate contamination from the LMXB, we considered offset pointing from the pulsar away from the LMXB. However, we calculated, and later confirmed with raster scans of the region, that this would have resulted in a net decrease in the signal to noise ratio.

The photon events from the two separate Experiment Data Systems (PCA/EDS) configurations were separately analyzed and fed into the “fasebin” ftool. This package handles the solar system barycentric corrections of the arrival times of the photons (via the JPL DE200 solar system and the RXTE orbital ephemerides), and then epoch-folds the data according to a supplied pulsar ephemeris. The radio pulsar ephemerides used in the epoch folding program, kindly supplied by V. Kaspi et al, are displayed in Table 2. The radio observations ruled out any sudden period jumps of the pulsar spin period (glitches) near or in between the two epochs of RXTE observations, which are separated by nearly six months. Other ftools packages allow manipulation of the epoch folded phaseogram according to spectral channels, binning in adequate number of phase bins etc. The epoch folded phaseogram of these events is displayed in Figure 2. The origin of the phaseogram corresponds to the absolute phase of the radio pulse. There is no compelling evidence for pulsed emission at the pulsar period. Note that the reduced  $\chi^2$  per degree of freedom (19 degrees of freedom) for the histogram displayed in Figure 2 is 1.99. This means that a random set of fluctuations consistent with a uniform background of the zero level shown (corresponding to 94.16 cps), i.e. the absence of a pulsation at the radio folding period, is ruled out at a 99.25 % confidence level. Currently we can only obtain the following  $2\sigma$  upper limit to the *pulsed* flux, based on the total observation of 132 ks, in the energy interval  $9 \text{ keV} < E_\nu < 18.5 \text{ keV}$  band (Ulmer et al 1991): :

$$UL = \frac{2}{\Delta E} \frac{\sqrt{C_{tot}}}{(A_{eff}t)} \sqrt{\frac{\beta}{1-\beta}} = 10^{-6} \text{ photons cm}^{-2}\text{s}^{-1}\text{keV}^{-1}$$

where we have taken the pulsar duty cycle  $\beta = 1/2$  and the RXTE effective area  $A_{eff}$  to be 6000  $\text{cm}^2$ . This upper limit is shown together with the detections and upper limits of PSR B1706-44 in other energy bands in Figure 3.

#### 4. Implications of multiband spectra for theoretical models:

The photon spectrum shown in Figure 3 from the ROSAT (keV) band to the TeV band has implications for theoretical models of pulsar radiation mechanisms. High energy electromagnetic radiation from pulsars is due to relativistic electrons and positrons which are accelerated in the magnetosphere surrounding the neutron star. The models for magnetospheric accelerators fall into two main classes depending upon their location with respect to the neutron star. In the polar cap model invoked originally to power radio emission from a pulsar (Ruderman and Sutherland 1975; Daugherty and Harding 1982) the acceleration zone for the primary electrons (positrons) is relatively close to the neutron star surface. The outer magnetospheric accelerators (Holloway 1973; – the “outer gap”), proposed for energetic photons (Cheng, Ho, & Ruderman 1986a,b, hereafter CHRa and CHRb), accelerate particles at a distance which is a good fraction of the light cylinder radius from the neutron star. As extensive  $e^\pm$  flows are generated by both polar cap and outer-gaps, the pairs from one would be expected to quench the other, and it is difficult to expect that both could survive on the same field lines, unless the field lines threading the two acceleration zones have differing curvatures and signs of net charge density etc. (see Wang et al 1998 for a discussion).

Currently, there are several different versions of the outer gap model in the literature which differ in significant detail as to the mechanisms of gap discharge through  $e^\pm$  pair production and the process of electromagnetic radiation emitted by these relativistic particles. The classic version of the CHR model is now extended by Zhang and Cheng (1997), Cheng and Ding (1994) as well as by Wang et al (1998). In addition there are variants of the classic outer gap model by Romani(1996) and Romani and Yadigaroglu (1995) who consider only the outwardly flowing  $e^\pm$  pairs and compute curvature, synchrotron and inverse Compton spectra from primary and secondary particles.

In polar cap models, primary particles are accelerated near the surface of the neutron star and produce  $\gamma$ -rays through curvature radiation and inverse-Compton emission. These  $\gamma$ -rays convert to electron-positron pairs in the strong magnetic field, initiating electromagnetic cascades as the pairs radiate synchrotron  $\gamma$ -rays which produce further pair generations. The X-ray and  $\gamma$ -ray spectrum from such a cascade initiated by curvature radiation was computed by Daugherty & Harding (1996) for the parameters of the Vela pulsar.

As already discussed, the rotation powered pulsars emit X-rays which are a combination of differing amounts of three spectral components: 1) power-law emission, resulting from non-thermal radiation of particles accelerated in the pulsar magnetosphere, 2) soft blackbody emission from surface cooling of the neutron star, and 3) a hard thermal component from heated polar caps. In addition, spectra may include a background of unpulsed emission from a synchrotron nebula. Clearly, component 1) relates most directly to the pulsar particle acceleration models. However, components 2) and 3) can also be indirectly related to the magnetospherically accelerated particles under certain circumstances, especially if they are seen as a pulsed component. The nebular background is due to energetic particles injected in the surrounding nebula outside the light cylinder. While the study of its properties is interesting in its own right (for example, to determine the injected particle spectrum and the strength of the nebular magnetic field - see Harding and De Jager 1997), for the purposes of detecting pulsed emission, it is a background component.

#### 4.1. Multi-waveband spectra and the non-thermal component of pulsed emission

Figure 3 shows the pulsed photon spectrum of PSR B1706-44 from EGRET detections in the hard gamma-ray bands as well as numerous upper limits in the soft and hard X-ray bands and TeV gamma-rays. Since  $P$  and  $\dot{P}$  for PSR B1706-44 are very close to those of Vela, the cascade spectrum of the two pulsars in the Polar Cap model is expected to be similar. We have plotted the Vela cascade spectrum of the PC Model (DH96 and Daugherty and Harding, in preparation) in Figure 3, extended down to 1 keV, and normalized to the PSR B1706-44 EGRET data points. In the Vela cascade model, the primary electrons are assumed to begin their acceleration above the surface at a height of 2.0 stellar radii. The acceleration zone extends to a height where the electrons have achieved an energy of 10 TeV and the cascade begins near the top of the acceleration zone. Acceleration starting at some height above the surface is likely, due to the screening of the parallel electric field near the surface by the cascades from returning positrons (see Section 4.2 and Harding & Muslimov 1998). The cascade spectrum is primarily synchrotron radiation from pairs, and has a high energy turnover around 3 GeV due to pair production attenuation in the local magnetic field. This turnover is quite sharp, because the pair production attenuation coefficient is an exponential function of photon energy, and thus no pulsed emission is expected at TeV energies. The spectrum has a low-energy break or turnover at the local cyclotron energy in the particle rest frame, blue-shifted by the particle energy. In this case, the local cyclotron energy in the particles' rest frame falls at 1.2 keV (the local field is  $10^{11}$  G) and the pairs have an average Lorentz factor of 50, giving a turnover energy of about 50 keV. Below the turnover, the spectrum flattens into a power-law formed by the broadening of the cyclotron fundamental by the pair energy distribution. This model spectrum falls just below the RXTE upper limit, indicating that the position of the cyclotron energy turnover is near its minimum acceptable value. The RXTE limit thus imposes a stringent upper limit on the emission radius in the polar cap model. For PSR B1706-44, the emission must occur within 2 stellar radii of the neutron star surface.

In the CHRa,b model the pair production and radiation mechanisms in the outer gap for Crab and Vela type pulsars are different although it was shown subsequently that different angles of inclination between the spin and magnetic axes can alter the picture substantially (Chen and Ruderman 1993). In the CHR model the synchrotron radiation from secondary  $e^\pm$  pairs generated in the outer gap (by the collision of the primary photons and the tertiary IR photons) is responsible for the photon spectrum in the 100 keV to 3 GeV range. The pulsed photon spectrum for Vela type pulsars (with  $P \geq P_t = 4.6 \times 10^{-2} B_{12}^{2/5}$  s) in the gamma-ray region is given by Cheng and Ding (1994) (see also Ruderman and Cheng 1988) as :

$$\frac{d^2 N_\gamma}{dE_\gamma dt} \sim \begin{cases} \exp(-E_\gamma/E_{max}), & \text{for } E_\gamma \geq E_{max}, \\ E_\gamma^{-3/2} \ln(E_{max}/E_\gamma), & \text{for } E_{min} \leq E_\gamma \leq E_{max}, \\ E_\gamma^{-2/3}, & \text{for } E_\gamma \leq E_{min}. \end{cases}$$

where  $E_{max}$  and  $E_{min}$  are given by:

$$E_{max} \sim 3/2 \gamma_{max}^2 \sin\theta \hbar\omega_B \simeq 7.5 \text{ GeV}$$

and  $E_{min}$  is given by:

$$E_{min} \simeq 3/2 \gamma_{min}^2 \sin\theta \hbar\omega_B \simeq 11 \text{ MeV}$$

for PSR B1706-44. Here  $\sin \theta$  is the mean pitch angle for the synchrotron emitting secondary particles and  $\gamma_{max}$  corresponds to the maximum energy of the secondary pairs, while  $\gamma_{min}$  corresponds to the secondary energy at which the radiative loss equals the magnetospheric crossing time and  $\omega_B$  corresponds to the local cyclotron frequency. The above outer gap spectrum is also plotted as a dashed line in Fig 2 and falls well below the RXTE limit when normalized to the EGRET points. Specifically, Cheng and Ding quote the  $E_{min}$  for Vela and PSR B1706-44 as (11MeV, 1.6 MeV) and  $E_{max}$  as (7.5 GeV, and 0.7 TeV) respectively. Although the  $E_{min}$  of the two pulsars which have very similar periods and magnetic fields are within an order of magnitude, no clear explanation is given as to why the  $E_{max}$  of the two pulsars differ by nearly two orders of magnitude, especially with the same or similar pitch angle distributions of the secondary particles. Physically, the upper spectral break ( $\hbar\omega_{max}$ ) in the CHR models comes from the maximum energy of the outer gap  $\gamma$ -rays which create the energetic  $e^\pm$  pairs whose synchrotron radiation is in the  $\gamma$ -ray/X-ray regime. The lower spectral break is related to the finite residence time (Ruderman and Cheng 1988) of the synchrotron radiating pairs on the open field lines of an outer magnetosphere such that they leave the magnetosphere (light cylinder) radius before they have a chance to radiate away most of their energy. Since the  $e^\pm$  leaving the light cylinder cannot retain the memory of neutron star rotation, the radiation beyond the light cylinder will not be pulsed, hence the 3/2 power law pulsed synchrotron spectrum in this model is expected to be valid only above  $E_\gamma \geq E_{min}$  which is typically in the MeV energy range. (CHRb obtained the spectral break between 3/2 and 2/3 power around 100 keV, corresponding to a local magnetic field strength



of  $5 \times 10^3$  G). Note that Ruderman and Cheng (1988) give the upper and lower bounds as the following functions of the period of Vela-type pulsars:  $E_\gamma \leq \hbar\omega_{max} = 3 \times 10^9(0.09s/P)^{17}$ eV and  $E_\gamma \geq \hbar\omega_c \simeq 10^6(P/0.09s)^7$ eV respectively.

Presumably the higher value of  $E_{max}$  ( $= 0.7$  TeV) was chosen by Cheng and Ding (1994) because PSR B1706-44 does not appear to have a sharp high energy cutoff in the EGRET range. However, this choice of this high  $E_{max}$  also violates the upper limit of pulsed flux at somewhat lower energies around 250 GeV due to Chadwick et al (1997). We note that, if the EGRET gamma-ray photon spectrum is to be explained by a 3/2 power law below 3 GeV due to synchrotron radiation from the secondary  $e^\pm$  pairs in the outer magnetosphere, as in CHR or Cheng and Ding, then the observed break in the power-law spectrum of PSR B1706-44 in EGRET data around 3 GeV might indicate an  $E_{max}$  close to that of the Vela pulsar as reported in Cheng and Ding (7.5 GeV).

The break in the photon spectrum at 3 GeV implies that (given a canonical maximum energy of the primary photon of  $10^7$  MeV), the innermost region of the magnetosphere where the production of the “synchro-curvature” photons from the secondaries are taking place (see Zhang and Cheng 1997) is typically at a local magnetic field of several times  $10^6$  gauss, i.e at about 100 stellar radii (or 1/5 of the light cylinder distance) for PSR B1706-44. For moderately inclined pulsars, this inner boundary of the outer gap would imply an inclination angle  $\chi$  ( $\cos\chi = \hat{\mu} \cdot \hat{\Omega}$ ) derived from the expression due to Halpern and Ruderman (1993):  $r_i \simeq 4/9 \cot^2 \chi (c/\Omega)$ , to be around 60 degrees.

If the EGRET detected fluxes are indeed described by a 3/2 power law below 3 GeV, then it appears that to accommodate the RXTE upper limit obtained in this paper, one requires a break in the photon spectrum at energies higher than about 50 keV (see Fig 3). As already mentioned, the PC model spectrum, if fitted to the EGRET pulsed fluxes, cannot extend to the keV regions unless there is a break as mentioned here. The outer gap model’s prediction due to Cheng and Ding (1994) (which has a slope of 2/3 with a spectral break at 1 MeV) as shown by a dashed line in Fig 3, passes well below the RXTE upper limit and is not constrained by it.

In a modification of the outer gap model (Wang et al 1998) the inward directed  $\gamma$ -ray curvature photons (of energy  $\sim 100$  MeV, instead of the much higher energy photons of energy  $\sim 10^7$  MeV as in the CHR version) radiated by the inward directed primary particles produce  $e^\pm$  pairs in the stronger magnetic field ( $10^{10}$  G) near the neutron star surface. The radius of the magnetic pair production (at about 5 stellar radii) is large compared to what is invoked in polar cap models. It is to be noted that the region of pair production and subsequent X-ray and low energy  $\gamma$ -ray emission is much closer to the neutron star (and is directed starward) than the high energy emission in the earlier CHR version of the outer gap model. Wang et al give a photon spectral index of 3/2 with lower and upper cutoff energies at 0.1 keV and 5 MeV respectively. We note that such a component is unlikely to be a continuation of the 3/2 power law photon spectrum from the EGRET energy bands, as such an extension would violate the RXTE upper limit as noted

above and the lower cutoff of 0.1 keV can be ruled out for an extrapolated EGRET spectrum. On the other hand, such a power-law component can be present with a lower strength, in addition to the same power law component (due to outwardly directed particle flux) as previously discussed by Ruderman and Cheng (1988) (see also Cheng and Ding 1994) if the latter is taken to describe the EGRET spectrum below  $\sim 3$  GeV. Since the former component is generated by a starward directed beam of gamma-rays, to be observable this X-ray component would come from the side of the magnetosphere opposite to the observer direction. The two components (outwardly directed X-ray and  $\gamma$ -ray beams and starward directed beams) will be separated in pulsar spin phase, possibly with different strengths in the X-ray bands and with different spectra below  $\sim 1$  MeV. These could be seen in phase resolved spectra should such spectra be available in the future.

#### 4.2. Polar cap heating by returned particles in PC and OG models & X-ray spectrum

In Fig 4 we have plotted an expanded view of the X-ray spectrum expected from the non-thermal emission from the PC and OG models, as discussed above, and the thermal radiation from the heated polar cap due to returned energetic particles from the acceleration regions. Also shown are the upper limits to the pulsed fluxes from ROSAT PSPC, ROSAT HRI, ASCA, XTE and OSSE (see Thompson et al 1996 for the references to these works; the ROSAT HRI limit is due to Finley et al, 1998). The ROSAT PSPC upper limit corresponds to the 18% modulation of the total flux reported by Becker et al (1995) (with a reported spectral index of  $\alpha = 2.4$  in the 0.1 - 2.4 keV band) while the ROSAT HRI upper limit corresponds to the upper limit of the pulsed flux as reported in Finley et al (1998) in the same band (we assume the same photon spectral index here as in Becker et al. (1995)). The ASCA upper limits are due to the fluxes in the 0.7 - 2.0 keV and 2.0 - 10.0 keV bands and their photon index of the combined SIS and GIS data ( $\alpha = 1.7$ ) as reported in Finley et al (1998). The RXTE upper limit in the 9.0 to 18.5 keV regime reported here is centered on a photon energy of 12.8 keV. The OSSE upper limit is due to Schroeder et al (1995).

The Polar Cap and the Outer Gap models have different predictions of the returned  $e^\pm$  particle flux reaching the surface of the neutron star. If the particle fluxes indeed translate proportionally to the *observable* X-ray luminosities, then these models could potentially be distinguished if the associated hot thermal pulsed component in the X-rays from the heated polar caps are detected and are distinguishable from the the soft thermal component due to the cooling neutron star. In the Polar Cap model, an accurate determination of the fraction of backflowing positrons generated in the pair formation fronts requires a self-consistent calculation of the screening of the electric field component parallel to the local magnetic field due to the cascade pairs and its feedback on the pair spatial distribution. The generated positrons which are turned around slightly suppress the voltage all the way down to the bottom of the polar magnetic flux tube, so that the accelerating electric field ( $\mathbf{E} \cdot \hat{\mathbf{B}}$ ) component vanishes at a height above the stellar surface rather than at the

actual surface. This is effectively an enhancement of the maximum number of electrons to be injected into the acceleration region. There is a maximum possible power in the backflowing positrons that will not shut off the parallel electric field. This will lead to the polar cap heating luminosity estimated by Harding and Muslimov (1998; HM98) as:

$$L_{e^\pm}^{max} \simeq \lambda_{max} L_{sd}$$

where  $L_{sd}$  is the spin down power of the pulsar and  $\lambda_{max} \simeq (3 \times 10^{-4} - 2 \times 10^{-2})(\kappa/0.15)^2$ , and  $\kappa = \epsilon I/MR^2$ , I, M, R being the moment of inertia, mass and radius of the neutron star and  $\epsilon \sim O(1)$ . If the X-ray emission is beamed into a solid angle of  $4\pi$  steradian, the X-ray emission due to returning particle flux gives rise to a hot polar cap temperature of:

$$T_{pc} = \left[ \frac{\lambda_{max} L_{sd}}{\sigma 4\pi R^2} \right]^{1/4}$$

where R is the radius of the heated polar cap. Taking  $R = R_0 \theta_{pc} = 4.5 \times 10^4 \text{cm}$ , the standard polar cap radius for the period of PSR B1706-44, and  $\lambda_{max} = 3 \times 10^{-4}$ , the backflowing positrons in the polar cap model are expected to produce a luminosity of  $1.0 \times 10^{33} \text{ erg s}^{-1}$  beamed into a solid angle of  $4\pi$  steradian with a polar cap temperature of  $5 \times 10^6 \text{ K}$ . In Fig 4, we have plotted the blackbody curve corresponding to  $\lambda = 3 \times 10^{-4}$  for the heated polar cap (hard) thermal radiation - the maximum flux expected from PSR B1706-44 on the basis of returned positron current as in HM98. This curve lies significantly above the ROSAT HRI and ASCA limits, implying a returning particle luminosity fraction much less than the maximum theoretically allowable.

Wang et al (1998) have argued that the X-ray emission properties of  $\gamma$ -ray pulsars differ from those that are not observed to be strong  $\gamma$ -ray emitters. For the gamma-ray pulsars, with accelerators presumably at very many stellar radii (“outer gap”) above the neutron star surface, curvature radiation gamma-rays moving starward produce a dense blanket of  $e^\pm$  pairs on closed field lines around the star. The pair blanket affects the X-ray emission properties by a) producing a nonthermal synchrotron spectrum with photon power law index of 3/2 between  $0.1 \text{ keV} \leq E_X \leq 5 \text{ MeV}$ , as discussed above, whose intensity (typically  $\sim 10^{33} \text{ erg s}^{-1}$ ) depends upon the backflow current and b) forming a cyclotron resonance blanket around the star, which shields the direct observation of hard X-ray thermal emission from the heated polar cap except through two narrow holes along the open field lines threading the polar caps. Less strongly modulated, softer X-rays can also escape by diffusing through the cyclotron resonant blanket. The ratio of the hard radiation flux from the heated polar cap coming through the holes ( $f_h$ ) to the flux through the blanket itself is given by Wang et al (1998) as:  $f_h/f_b = r\Omega(\tau_b + 1)/2c$ , where the expected optical depth  $\tau_b$  is roughly 10-200 and the blanket area is roughly  $10^3$  times greater than the hole size. Therefore the radiation flux leaking through the holes may be  $10^{-2}$  to 0.2 times the more uniformly distributed softer flux escaping from the blanket. With constant bombardment of the relativistically inflowing particles at a rate of  $10^{32} \text{ s}^{-1}$  (the Goldreich-Julian current) which radiate away much of their energy before they reach the polar cap, Wang et al

estimated a total X-ray luminosity of  $L_x = fE_f\dot{N}_0 \simeq 2.1 \times 10^{32} \text{erg s}^{-1}$ , where the factor  $f$  is the fraction of Goldreich-Julian current  $\dot{N}_0$  that flows back through the outer gap accelerator to the polar cap (taken to be  $1/2$  for  $\gamma$ -ray pulsars not too far from their death lines). Here,  $E_f = mc^2 [2\Omega e^2/(mc^3)\ln(r_{LC}/R)]^{-1/3} \sim 5.5 \text{ erg}$ , is the residual energy of the charged particles impacting the polar cap. Using this luminosity and the above range of the fractional flux ratio  $f_h/f_b \simeq (0.01 - 0.2)$  for the open field lines bundle for PSR B1706-44, the resultant hard X-ray (thermal) component, should the beam intercept the observer, would translate to a photon flux of

$$F_\nu(T) = (0.01 - 0.2) \frac{1.82 \times 10^{-2} E_{keV}^2}{\exp[E_{keV}/(T/2 \times 10^6)] - 1}$$

photons  $\text{cm}^{-2} \text{s}^{-1} \text{keV}^{-1}$

Here, the heated polar cap temperature for PSR B1706-44 is taken as the same as that predicted for PSR0656+14, by Wang et al (1998), namely  $2 \times 10^6 \text{ K}$ .

The range of the heated polar cap fluxes corresponding to the above range of  $f_h/f_b$  is shown as the shaded area in Fig 4. Note that the available observational upper limits are also constraining the extent of the heated polar cap emission in both PC and OG models by limiting  $\lambda$  or  $f_h/f_b$ . The upper range of  $f_h/f_b$  is ruled out by the ROSAT HRI limit requiring that all but about 1 % of the returned particle luminosity must be hidden at the hard X-ray and redistributed at lower bands. The ROSAT and ASCA limits restrict  $\lambda$  ( $\leq \lambda_{max}$ ) in the PC model to a value less than  $10^{-5}$ , the observed limit for the Vela pulsar.

### 4.3. Optical band luminosity predictions in OG model and R-band observation

Zhang and Cheng (1997) using the classic thin outer gap models of CHR give an implied IR luminosity of the tertiary photons for Geminga. Using the same line of argument, we can estimate that PSR B1706-44 should show a total IR band luminosity of

$$L_{IR} = n_{IR} \Delta\Omega R_L^2 c E_{IR}$$

$$\sim 3 \times 10^{33} (P/0.102s) (\Delta\Omega/1sr) (E_{IR}/0.01eV) \text{ erg s}^{-1}$$

should the tertiary photons indeed play a crucial role in sustaining the  $e^\pm$  discharges through IR- $\gamma$ -ray photons collision (the latter in turn produced by inverse Compton scattering of the same IR photons by highly energetic primary electrons). Chakrabarty and Kaspi (1998) have found an upper limit to the R-band magnitude for a region coincident with the pulsar of 18 mag, corresponding to a flux of  $2.4 \times 10^{-13} \text{erg s}^{-1} \text{cm}^{-2}$  at  $0.7 \mu\text{m}$ , which translates to an R-band total luminosity of  $9 \times 10^{31} \text{erg s}^{-1}$  at the pulsar. If the spectrum at the IR wavelengths is adequately described by a Rayleigh Jeans spectrum, then the corresponding flux limit from the R-band upper limit is well below the theoretical IR luminosity predicted from the thin

outer gap model. Inconsistencies between the IR luminosity required by outer gap models and observed IR limits (IRAS) for other pulsars has been pointed out by Usov (1994), Zhang and Cheng(1997). The R-band upper limit corresponding to 18 mag, however is not sufficiently constraining compared to the scaling of the optical vs gamma-ray luminosities expected in outer gap models (CHR) as given by Usov (1994, see his equation (24)). Given a pulsed gamma-ray flux of  $3 \times 10^{13}$  JyHz at  $10^{24}$  Hz (Thompson et al 1997), Usov predicts an optical flux of  $F_{opt} \geq 4 \times 10^{-4} F_{\gamma} \simeq 1.2 \times 10^{-13}$  erg s<sup>-1</sup> cm<sup>-2</sup> for CHR outer gap models. However, the more stringent (possible) upper limit of 21 mag quoted by Chakrabarty and Kaspi (1998) would violate the expected optical flux in the outer gap model.

## 5. Conclusions:

The main outcome of our work has been to provide an upper limit of the pulsed X-ray flux in the 9-18 keV band which constrains any non-thermal emission spectrum extending from EGRET gamma-ray bands towards the soft X-ray bands of ROSAT. In particular, the cyclotron turnover required for the Polar Cap model downwards of 50 keV, restricts the height of polar cap acceleration to less than two stellar radii above the NS surface. On the other hand, if a break in the EGRET spectrum around 3 GeV is to be consistent with the spectra at lower energies, then the boundary of the outer gap acceleration zone nearest to the neutron star would be nearly 100 stellar radii away. In particular, our RXTE limit would tend to rule out a particular component of the outer gap model emission (starwardly directed beam of curvature gamma-rays materializing in relatively strong magnetic field to produce secondary e<sup>±</sup> that synchrotron radiate to produce the power law X-ray gamma-ray spectra) requiring a lower cutoff of 0.1 keV, unless it is a weaker component that is below the extrapolation from the EGRET spectrum to lower energy bands. Future phase resolved spectra of this pulsar might therefore have information to reveal with regard to the nature and strength of these possibly different components tied to different mechanisms.

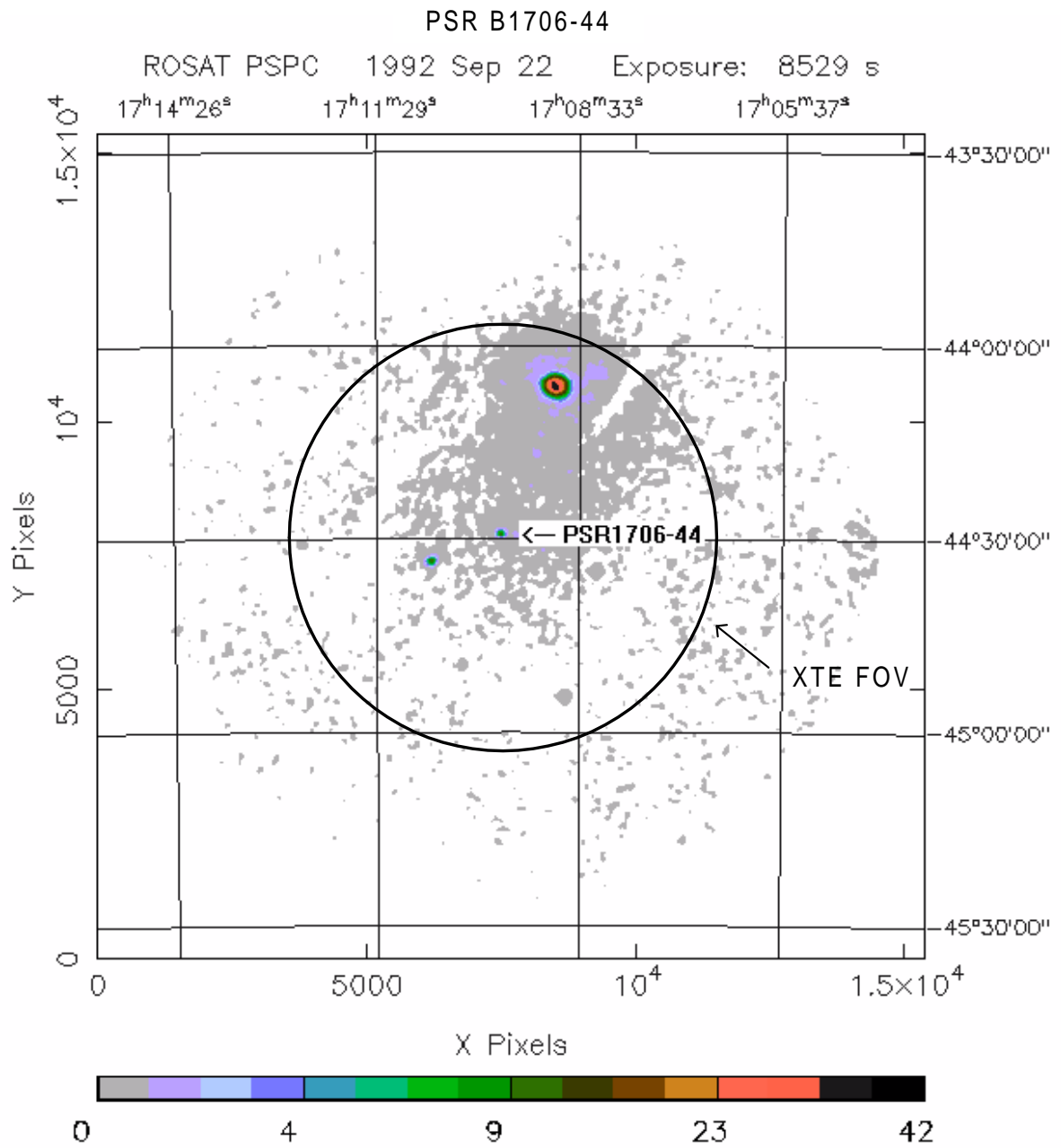
## 6. Acknowledgments:

We thank V. Kaspi, M. Bailes, N. Wang and R.N. Manchester for providing the radio ephemerides of PSR B1706-44 measured from ATNF. We thank D.J. Thompson and Arnold Rots for discussions and for the compilation of data on this pulsar at other energy bands and the staff of XTE Guest Observer Facility for help with data analysis. A.K.H. thanks Joe Daugherty for assistance in producing the polar cap model cascade spectrum. A.R. acknowledges support through a Senior Research Associateship of the National Research Council at NASA/Goddard and the RXTE Guest Observer program.

## REFERENCES

- Arons, J. 1981, ApJ 248, 1099.
- Becker, W., and Trümper, J. 1997, A & A. 326, 682.
- Becker, W., Brazier, K.T.S. and Trümper, J. 1995, A & A. 298, 528.
- Chadwick, P.M. et al 1997 Proc. 4th Compton Symp., Williamsburg, (ed C. Dermer, M.S. Strickman and J.D. Kurfess; AIP Proc 410).
- Chakrabarty, D. and Kaspi, V. M. 1998, LANL e-print astro-ph/9801017 v2.
- Chen, K.-Y. and Ruderman, M.A. 1993, ApJ 408, 179.
- Cheng, K.S. and Ding, W. K.-Y., 1994, ApJ 431, 724.
- Cheng, K.S., Ho, C. and Ruderman, M.A. 1986, ApJ 300, 500 (CHRa).
- Cheng, K.S., Ho, C. and Ruderman, M.A. 1986, ApJ 300, 522 (CHRb).
- Daugherty, J.K. and Harding, A.K. 1982, ApJ 252,337.
- Daugherty, J.K. and Harding, A.K. 1996, ApJ 458, 278.
- Fierro, J. 1995, Ph.d. Thesis, Stanford University, Palo Alto.
- Frail, D.A., Goss, W.M., and Whiteoak, J.B.Z. 1994, ApJ 437, 781.
- Finley, J.P., Srinivasan, R., Saito, Y., Hiriyama, M., Kamae, T., and Yoshida, K., 1998 ApJ 493, 884.
- Halpern, J. and Ruderman, M.A. 1993 ApJ 415, 286.
- Harding, A.K., and Muslimov, A. 1998, Ap J, submitted.
- Harding, A.K. and De Jager, O. 1997, Proc of Kruger National Park Workshop on TeV astronomy.
- Ho, C. 1989, ApJ 342, 396.
- Holloway, N.J. 1973, Nature, 246,6.
- Johnston, S., Lyne, A.G., Manchester, R.N., Kniffen, D.A., D’Amico, N., Lim, J. and Ashworth, M. 1992, MNRAS, 225, 401.
- Nel, H. et al 1996 ApJ, 465, 898.
- Ray, A., Harding, A.K. and Strickman, M.S. 1997 in Proc of 4th Compton Symp, Williamsburg, (ed C. Dermer et al, AIP Proc 410).
- Ray, A. and Benford, G. 1981, Phys Rev D, 23, 2142.
- Romani, R.W. 1996, ApJ 470, 460.
- Romani, R.W. and Yadigaroglu, I.-A. 1995, ApJ 438, 314.
- Ruderman, M.A. and Cheng, K.S. 1988, 335, 305.
- Ruderman, M.A. and Sutherland, P.G. 1975, ApJ 196, 51.

- Sturmer, S.J. and Dermer, C.D. 1994, ApJ 420, L79.
- Thompson, D.J. 1996, in Pulsars: Problems & Progress (eds S. Johnston et al) Astron Soc Pacific Ser. 105, 307.
- Thompson, D.J. et al 1997, in Proc of 4th Compton Symp. Williamsburg, (ed C. Dermer et al, AIP Proc 410).
- Schroeder, P.C., Ulmer, M.P., Matz, S.M., Grabelsky, D.A., Purcell, W.R., Grove, J.E., Johnson, W.N., Kinzer, R.L., Kurfess, J.D. and Strickman, M.S. 1995, ApJ, 450, 784
- Ulmer, M.P., Purcell, W.R., Wheaton, W.A. and Mahoney, W.A. 1991, ApJ 369, 485.
- Usov, V.V. 1994, ApJ 427, 394.
- Wang, F.Y.-H., Ruderman, M., Halpern, J.P., and Zhu, T. 1998, Columbia University preprint.
- Zhang, L. and Cheng, K.S. 1997, ApJ 487, 370.



corcoran 20-Feb-1997 11:59

Fig. 1.— X-ray sky around PSR1706-44 and the RXTE Field of View.



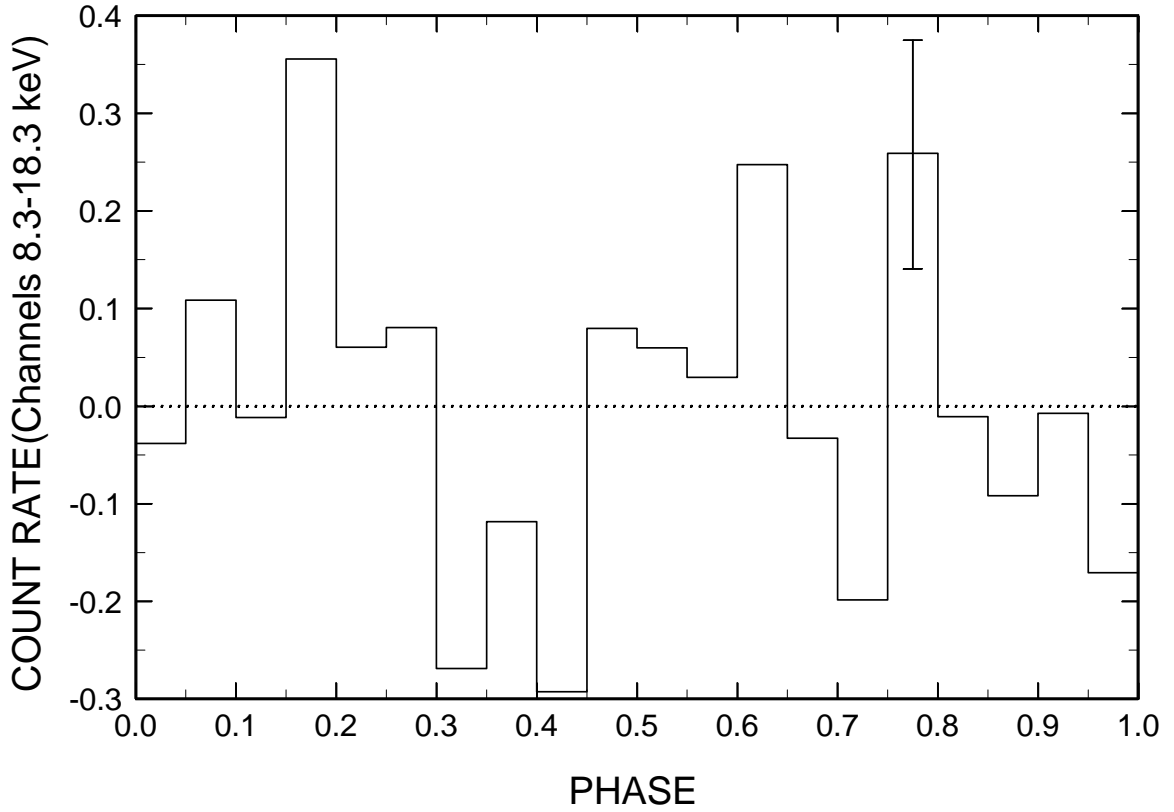


Fig. 2.— PSR1706-44 phaseogram (channels corresponding to 8.3-18.3 keV) epoch folded according to pulsar ephemerides. Average count rate in the phase interval  $0.0 < \phi < 1.0$  (marked as 0 on the y-axis) corresponds to 94.2 counts/s; the  $1 \sigma$  error bar in the individual bins is 0.12 cts/s. X-ray bursts of neighboring lmx b 4U1705-44 have been excluded from the data. Net exposure is 132ks.

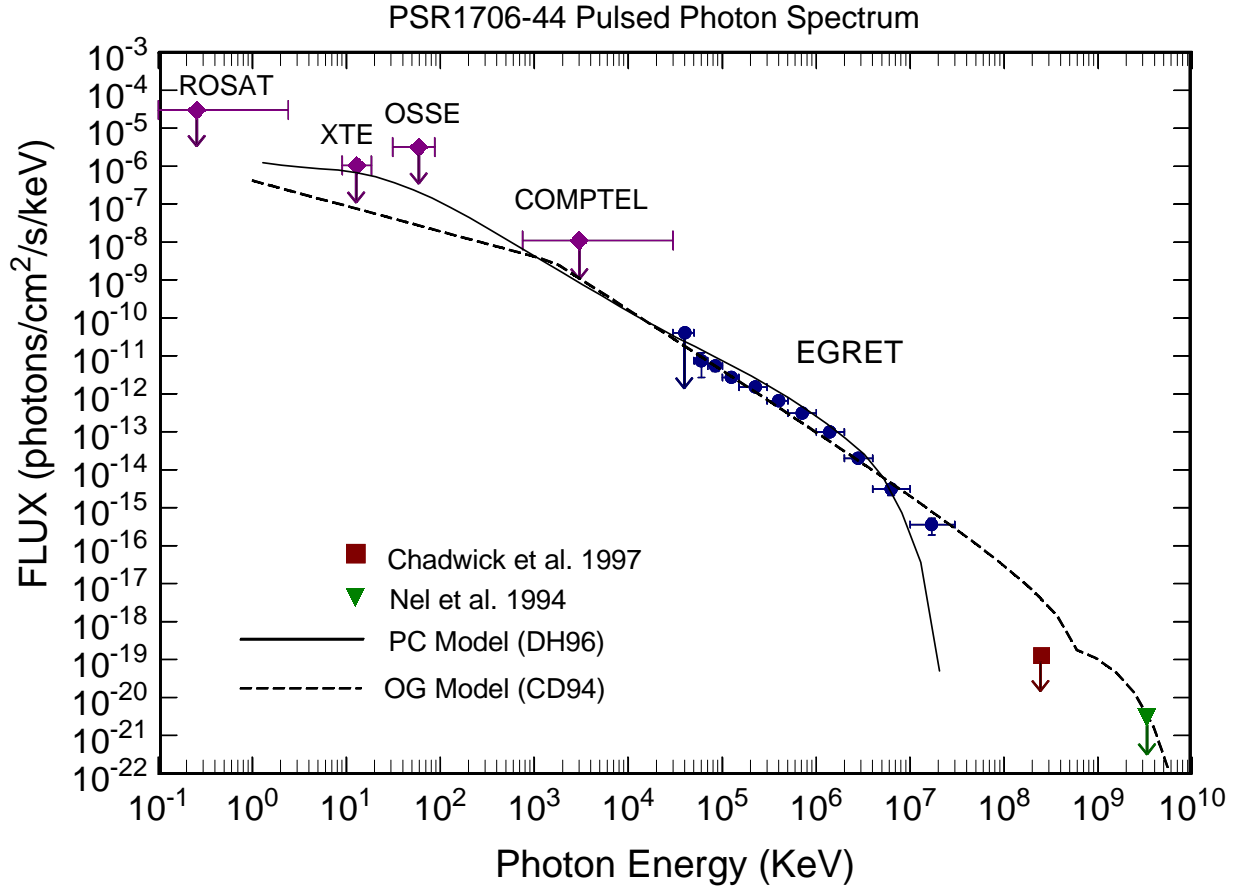


Fig. 3.— PSR 1706-44 pulsed photon spectrum, including upper limits, in the X-ray and gamma-ray bands. Also shown are the predictions of the Polar Cap and Outer Gap models. For references to the data points see Thompson et al (1996) and Finley et al (1998).

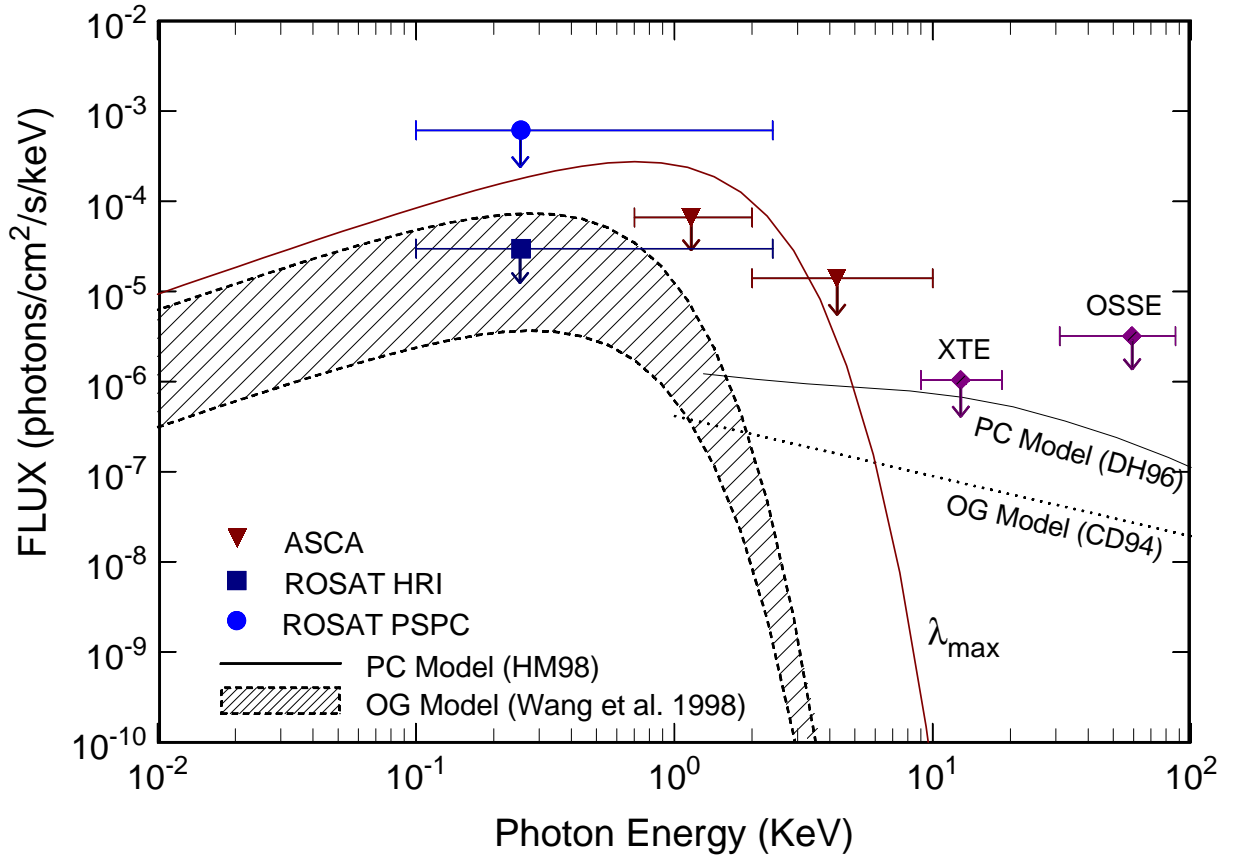


Fig. 4.— PSR 1706-44 pulsed photon flux upper limits, in the X-ray band. Expected blackbody spectra from heated polar cap due to inflowing energetic particle flux are shown for Polar Cap and Outer Gap models. Also shown are the predictions of nonthermal emission (see Fig. 3).

Table 1: Summary of RXTE Observations of PSR B1706-44

Observation Date	Beginning MJD	PCA/EDS Configuration	Total Live Time(s)
1996 Nov 9 & 11	50396.371	GoodXenon	33487
1996 Nov 10 & 11	50397.922	E_125us_64M_0-1s	52162
1997 May 16 - 19	50584.581	GoodXenon	45776

Table 2: Radio Pulsar Ephemerides used in Epoch Folding<sup>†</sup>

Epoch JD	Range of fit JD	$\nu_0$ Hz	$\dot{\nu}$ $s^{-2}$	$\ddot{\nu}$ $s^{-3}$
50273.000000458	50114-50433	9.7598013942166	-8.85435D-12	1.47D-22
50588.000000129	50563-50613	9.7595604761275	-8.84955D-12	0.00D-00

<sup>†</sup> Courtesy: V. Kaspi, M. Bailes, N. Wang & R.N. Manchester; RA, DEC (J2000) = 17 09 42.722, -44 29 8.44 (row 1); = 17 09 42.730, -44 29 8.30 (row 2).